ANALYSIS OF RESIDUAL STRESS BY X-RAY DIFFRACTION AND STUDY OF MICROSTRUCTURE IN WELDED JOINT OF ASTM A-36 MARINE STEEL

M. C. L. Souza[a],
I. P. Magalhães[a]
G.M. Silveira de Sá[a]
V. I. Monine[b]
R.S. Perez[c,d],
and N. C. O. Tapanes[a]

[a] State University of Rio de Janeiro
Av. Manuel Caldeira de Alvarenga, 1203, Rio de Janeiro - RJ, 23070-200, Brasil
mauro.souza@uerj.br
[b] Polytechnic Institute of the State of Rio de Janeiro. R. Hormindo Silva, 25 - Lagoinha, Nova Friburgo - RJ, 28625-570, Brasil
[c] RS PEREZ Náutica
Pr Sapinhoera Itaguaí- RJ, 23825-250, Brasil
[d] Federal University of Rio de Janeiro
Ilha do Fundão -RJ, 21941-901, Brasil

Received: Jun 03, 2023
Reviewed: Jun 18, 2023
Accepted: Jun 25, 2023

ABSTRACT

ASTM A-36 marine steel is one of the most used and classified as a medium strength carbon steel. Its characteristics and purpose are in common applications and in metallic structures in general, sawmills, walkways, agricultural machinery and implements, road, rail and oil implements. It is used in angles, round, flat and square bars and I, U and T profiles. In this work, 10 mm sheets, with a V chamfer, were welded using the MIG/MAG process and X-Ray Diffraction measurements were carried out to study of residual stresses caused by the welding process. Then samples were taken for metallography and microscopy in the Scanning Electron Microscope (SEM). They were also performed in the three regions of the weld: base metal (MB); thermally affected zone (ZTA) and in the molten zone (ZF) Brinell hardness tests, to determine the energy stored in the regions of the weld bead. Vickers Microhardness measurements were also made at the ZTA, as it is a very narrow range, to give more precision to the hardness measurements. The X-Ray Diffraction test showed that the air-cooled samples are compressive and the water-cooled samples are tensile. The micrographs of the samples, in the region of the weld, showed that the ferritic phase prevailed in the molten zone. It was also observed the precipitation of carbides and alloying elements, in addition to the presence of martensite. It is concluded, therefore, that the results for the MIG/MAG welding were satisfactory and recommended for the welding of ASTM A-36 Steel.

Keywords: Tensile Tests; X-ray Diffraction, Residual Stresses; Micrography

INTRODUCTION

The use of steel, in buildings and structures, in general, first appeared in England, over 200 years ago. Since then, it has been improving its technology and contributing to the development of the sector all over the world. In Brazil, the story is more recent. It was at the end of the 19th century and the beginning of the 20th century that steel began to be used, but still in the form of imported prefabricated structures to meet the growing demand for bridges and buildings.

Steel today is produced in a wide variety of applications. This variety arises according to the need to adapt to the requirements of specific applications that are emerging on the market, whether the chemical composition and final format. to its strength, ductility and other properties.

One of the most commonly used steels with these characteristics is the A36 steel, which is lightweight and has a low carbon content, used primarily as a structural material and also used in bars, angles and beams. It is relatively simple in chemical structure, which keeps its cost low. Soldering is very simple and, in general, very easy. It is a widely available steel and is standardized by the American Society for Testing and Materials (ASTM). (CBCA)

The present work evaluated the characteristics and reactions of A36 steel before a MIG/MAG welding process, through measurements of residual stresses, post-weld, by X-Ray Diffraction and also by optical microscopy tests, which evaluates the entire microscopic part of the soldered joint in order to reveal all the flaws produced during the soldering process.

MATERIAL AND METHODS

Material

Among the currently existing structural steels, the most used and known is ASTM A36, classified as a carbon steel of medium mechanical strength.

However, the modern trend towards using increasingly larger structures has led engineers, designers and builders to use higher strength steels, the so-called high strength and low alloy steels, in order to avoid increasingly heavier structures.
Table 1 lists the chemical composition and mechanical properties of a medium strength carbon steel (ASTM A36).

Table 1. Chemical Composition of Steel ASTM A26, % m/m.

C	Mn	S	P	Cu	Si
0.26	0.75	0.05	0.40	0.20	0.20

The Yield Limit of this steel is 250 MPa; o Resistance Limit 400-550 MPa and Elongation after rupture, lo = 20 mm, in 20 minutes.

High-strength, low-alloy steels are used whenever you want:

• Increase the mechanical strength by allowing an increase in the unitary load of the structure or making possible a proportional reduction of the section, that is, the use of lighter sections;
• Improve resistance to atmospheric corrosion;
• Improve shock resistance and fatigue limit;
• Raise the yield strength to tensile strength ratio without appreciable loss of ductility.

Among the steels belonging to this category, those of high strength and low alloy, resistant to atmospheric corrosion, deserve special mention. These steels were introduced to the North American market in 1932, with specific application in the manufacture of freight cars. Since its launch until today, other steels with similar behavior have been developed, which make up the family of steels known as weatherable. Framed in several norms, such as NBR 5008, 5920, 5921 and 7007 and the North American ASTM A242, A588 and A709, which specify limits of chemical composition and mechanical properties, these steels have been used all over the world in the construction of bridges , viaducts, silos, power transmission towers, etc. Their great advantage, in addition to dispensing with painting in certain environments, is that they have greater mechanical resistance than carbon steel. In extremely aggressive environments, such as regions with high sulfur dioxide pollution or those close to the coastline, painting gives them a performance superior to that given to carbon steel. (CBCA, 2014)

Welding

For the preparation of the samples, the ASTM 36A carbon steel plates were welded using the MIG welding process, at the Petrus Professional Training Center, the process being manual and in a vertical position, obtaining two samples. The first sample was slowly cooled to room temperature. The second was cooled in water at room temperature, and being continuously stirred until complete cooling.

X-Ray Diffraction Test

An ASTM A-36 steel strip measuring approximately 6x1cm was used, cut using a polycut machine, then sent for analysis of Residual Stress measurements by X-Ray Diffraction, using specific equipment, for such an analysis (CULLITY, 1978).

The procedures and tests were carried out using the program "Processing the diffraction line profile" developed by MONINE et al. (1994), based on the approximation of the experimental profile by analytical function. The stress measurement method by X-ray diffraction has been tested many times by stress measurements in the flexed sheets by comparing the values of applied stresses and those measured by X-ray diffraction (PUC-RIO, 2018; SÁ, 2011).

Residual stresses generated by the welding process were carried out in a mini X-ray diffractometer, with a position-sensitive X-ray detector and a special collimator with a tip at the end. The X-Ray Equipment was developed at the Laboratory of Physical Welding Tests at UFRJ (MONINE et al., 2001). Data processing based on approximation of the experimental DRX profile, by the modified Cauchy function, increases the precision and accuracy of stress measurements (ESTEFEN, et al. 2008).

The process consists of a tip that touches the weld of the sample steel, and a reading is automatically taken that is received by the program where it reads the residual stresses in the welded joint where it is possible to analyze the discontinuities of the material.

In this program it is possible to verify that there is a peak of the diffraction line determined by processing the line profile based on the approximation of the experimental profile by an analytical function.

Sample Preparation

The quality control of a metallurgical product can be structural and dimensional. The second is concerned with controlling the physical dimensions of a given product, called Metrology. The first is concerned with the material that forms the part, its composition, property, structure, application, etc. It can be: physical, chemical, metallographic and special. In this Material we will enunciate the Metallography practice with regard to sample preparation (ROHDE, 2018).

Sometimes it is necessary to partition the specimen to obtain samples that will serve for

metallographic analysis, but mechanical operations such as turning, planing and others, impose severe microstructural changes due to cold mechanical work. Abrasive cutting offers the best solution for this sectioning, as it completely eliminates cold mechanical work, resulting in flat surfaces with

low roughness, quickly and safely. The equipment used for cutting known as "cut-off", or polycutting, with intensely cooled abrasive discs (avoiding deformations due to heating) at relatively low speeds is widely used in metallographic laboratories.

Cutting Discs

They consist of fine abrasive disks (usually alumina or silicate oxide), aggregated with rubber or any other binder. The plate sample is shown in figure 1.

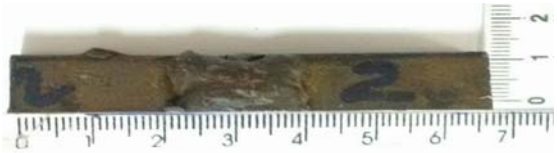

Figure 1 - ASTM A-36 steel sheet after cutting.

The choice and location of the section to be studied generally depends on the shape of the piece and the data that one wishes to obtain or analyze. In general, longitudinal cutting or transverse cutting is carried out on the sample.

The longitudinal section allows you to check:
• If the part is cast, forged or laminated;
• If the part was stamped or turned;
• Bar welding
• The extent of surface heat treatments, etc.

The cross-section allows you to check:
• The nature of the material;
• Homogeneity;
• The shape and dimensions of the dendrites;
• The depth of tempers, etc.

The sectioning of the sample must be carried out in such a way that it does not complicate the following operations. Among the cutting methods, the one most suitable for metallographic testing is wet abrasion cutting. In this case, the cutting discs are classified according to the hardness of the abrasive grains. During the cutting operation, the utmost care must be taken not to modify the structure of the specimen. The cut must never be continuous, so that excessive heating does not occur (above 100º C) due to lack of coolant penetration. Burr at the end of the cut should be avoided so that it does not make embedding difficult, if necessary, hence the need to use the appropriate disc according to the material to be cut. Due to its size and thickness mentioned in Figure 1, the steel sample did not need embedding to facilitate SEM reading.

Sanding

Due to the degree of perfection required in finishing an ideally prepared metallographic sample, it is essential that each preparation step is performed with care, it is one of the most time-consuming processes in metallographic sample preparation.

Operation that aims to eliminate scratches and deeper marks on the surface, giving a finish to this surface, preparing it for polishing. There are two sanding processes: manual (wet or dry) and automatic. The manual sanding technique consists of sanding the sample successively with sandpaper of increasingly smaller grain size, changing direction (90°) in each subsequent sandpaper until the traces of the previous sandpaper disappear. (ROHDE, 2010)

The most suitable sequence of sandpaper for metallographic work with steels is 100, 220, 320, 400, 600 and 1200 (There may be variations). In order to achieve an effective sanding, it is necessary to use the appropriate sanding technique, because according to the nature of the sample, the working pressure and the sanding speed, plastic deformations appear on the entire surface due to kneading and temperature increase. These factors can give a false image of the sample, so the following precautions must be taken:

•Appropriate choice of sanding material in relation to the sample and the type of final examination;
•The surface must be strictly clean, free of liquids and grease that could cause chemical reactions on the surface;
•Deep scratches that appear during sanding must be eliminated by sanding again;
•Different metals must not be sanded using the same sandpaper. In addition to sanding to prepare the sample for subsequent polishing, there is grinding or "Lapping", which makes use of loose abrasive grains rolling freely between its support and the surface of the sample.

Polishing

Post-sanding operation that aims at a polished surface finish free of marks, uses abrasives such as diamond paste or alumina for this purpose, in this sample the first option was used.

Before performing the polishing, the surface of the sample must be cleaned, in order to leave it free of abrasive traces, solvents, dust and others.

The cleaning operation can be carried out simply by washing with water, however, it is advisable to use liquids with a low boiling point of ethyl alcohol so that drying is quick.

Some grains and phases will be more attacked by the reagent than others. This causes each grain and

phase to reflect light differently from its neighbors. This enhances the contours and grain and gives different shades to the phases allowing their identification under the microscope.

Chemical Attack

The chemical attack aims to reveal the microstructure of a sample under the light of an optical microscope using chemical reagents. (FILHO, 2013) These reagents are basically diluted solutions of organic or inorganic acids, alkalis, or other solutions of a complex nature. The final selection of a solution to bring about development of the structure depends on the composition and structural conditions of the metal or alloy. (BAPTIST)

The surface of the sample, when attacked by specific reagents, undergoes a series of electrochemical transformations based on the oxidation-reduction process, whose contrast increase is due to differences in electrochemical potential. Local cells are formed where the chemically poor constituents act as an anode, reacting with the attack medium more intensely than the more noble ones.

For etching, aqueous or alcoholic solutions of acids, bases and salts, as well as molten salts and vapors are used. Contrast varies depending on chemical composition, temperature and time.

There are a huge variety of chemical attacks for different types of metals and situations. In general, the etching is done by immersing the sample for a period of approximately 10 seconds, so that the microstructure is revealed. One of the most commonly used reagents is NITAL, (nitric acid and alcohol), which works for the vast majority of ferrous metals. Table 2 shows the reagent and composition

Table 2 - Chemical Reagent for sample surface attack

Reagent	Composition	Application method	Indicated materials
NITAL 2.0	2ml HNO3 +98ml Ethyl Alcohol	Immersion	Carbom steel

Optical Microscopy

The microscopy of the samples was performed at UFRJ, using an Optical LED Microscope, 40X-2,500X, manufactured by OMAX.

RESULTS AND DISCUSSION

Measurement of Residual Voltages

Stress measurements in the weld bead are based on the determination of displacements of the diffraction line profile caused by the action of residual stresses.

Knowing the residual stresses in the weld bead is very important. Most of the destruction of welded joints takes place in it. The measurement methodology presented in Materials and Methods is based on the determination of displacements of the diffraction line profile caused by the action of residual stresses.

Carbon steel plates joined by the MIG welding process and cooled after welding in air (sample 1) and water (sample 2) were analyzed. The position of the diffraction line peak was determined by processing the line profile based on the experimental profile approximation by the Cauchy function, modified, which can be expressed by equation (1):

$$y(x) = 1/[1+a(x - b)^2]^n + 0{,}5/[1+a-b-\delta)^2]^n \qquad (1)$$

In equation (1) x, the angular coordinate and the first and second terms refer to the X-ray components called Ka1 and Ka2, normalized to 1 and 0.5, respectively, with a being the parameter responsible for the width of the diffraction line, δ the distance between the Ka1 and Ka2 components. The exponent n improves the Cauchy (Lorenzian) function, due to the fact that it can take not only a whole number, but also a fractional number. Thanks to this, the adjustment of experimental data can be carried out more accurately and reliably. Finally, the parameter b that determines the diffraction angle of the analyzed profile. whose calculation is the main objective of processing the experimental data of the diffraction test.

Diffraction lines obtained experimentally in the X-ray apparatus and processed by the program are shown in figures 2 and 3.

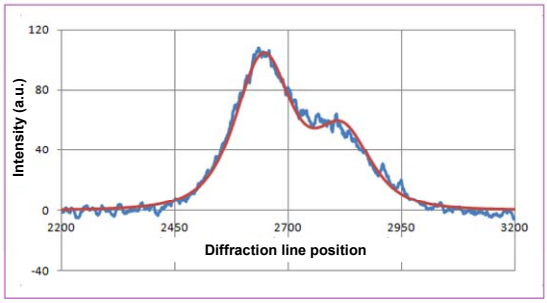

Figure 2 - Diffraction line profile of solder bead for air-cooled sample: blue - experimental profile; red - profile processed by the analytic function

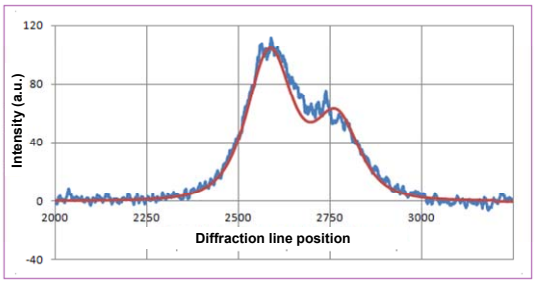

Figure 3 - Diffraction line profile of solder bead for water-cooled sample: blue - experimental profile; red - profile processed by the analytic function.

The comparison of the samples is based on the diffraction line obtained, where the sample cooled in air presented greater intensity at the point above 2600 (2540 and 2700) and the sample cooled in water presented greater intensity at the point below 2600 (2500 to 2750).

Optical Microscopy

The first photo (fig. 4) of the base metal, with a magnification of 50x, shows a ferritic structure, with some non-metallic inclusion bands, revealing a lamination product. As the Base Metal region is the farthest from the weld bead, it is almost unaffected by the heat zone induced during soldering. Thus, the structure resulting from the slow cooling of austenite below 727ºC, for a eutectoid steel is called pearlite. Pearlite is a structure made up of ferrite+cementite phases. Pearlite nucleates preferentially in the grain boundaries as it is possible to observe in the micrograph, the darkest region is the pearlitic structure, while the lighter one is the ferrite phase. Figure 5 shows with 200x magnification and in figure 6 with a magnification of 500x, a coarser structure of ferrite - cementite can be observed.

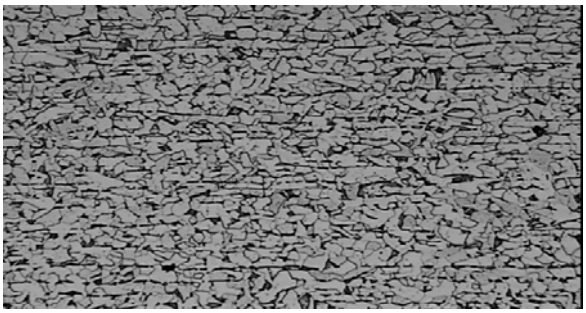

Figure 4 - Base metal microscopy (50x magnification)

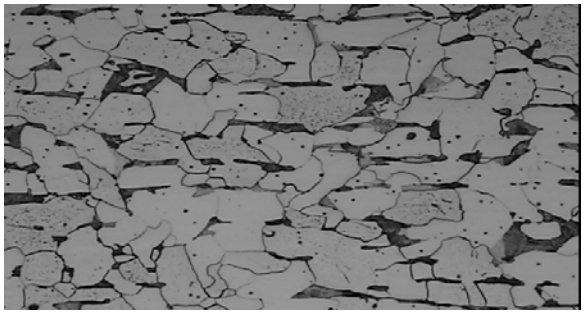

Figure 5 - Base metal microscopy (200x magnification)

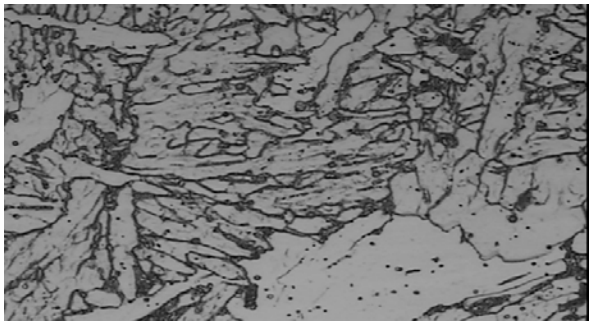

Figure 6 - Base metal microscopy (50x agnification)

Figure 7 shows a ferrite-pearlitic structure where pearlite begins to undergo a transformation at the top of the temperature reached, and a minimal region of pearlite, and with base metal on the right.
In continuously cooled steels, the increase in the cooling rate causes the pearlite to be formed at increasingly lower temperatures, causing a reduction in the interlaminar spacing. As it was possible to observe the evolution of the pearlitic structure in the HAZ region to the base metal region.

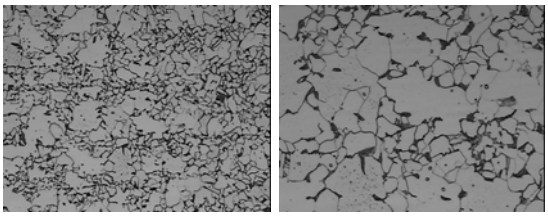

Figure 7 - Microscopy of the ZTA with magnifications: (a) 200x and (b) 500x

CONCLUSION

The results obtained by the measurements of Residual Stresses by X-ray Diffraction showed that the stresses of the air-cooled samples are Trative. The results obtained for samples cooled in water are Compressive. This is since the faster cooling, with Water, in the value of σres = + 0.85 MPa, causes much greater stresses in the microstructure of the welded steel, generating Compressive stresses which, in general, is better, since it does not generate cracks in the material. With air-cooled steel, the residual stresses are Trative, in the value of σres = - 70 MPa.

These tensions are not good, as they can generate cracks, which can make the material more fragile.

We can therefore conclude that the main cause of the appearance of residual stresses in the weld metal is associated with its contraction in the process of lowering the temperature, after crystallization, which generates the tensile stresses. However, cooling in water causes a quenching effect, causing compressive stresses. Obviously, the presence of compressive stresses is preferable from a practical point of view and this is what happened in the heat treatment performed.

The micrographs showed the maintenance of Perlite and Ferrite in the Base Metal, as expected for a low carbon steel.

Polygonal Ferrite, with lignet passes, is present in the Fused Zone of the weld

In the Thermally Affected Zone, the high heat generated Ferritic Pearlite, but there was no formation of Bainite, even with cooling in water.

ACKNOWLEDGEMENTS

The authors would like to thank the financial support given by the Research Support Foundation of the State of Rio de Janeiro (FAPERJ) to the study.

REFERENCES

ASTM A 36. Available in: <http://www.astm.org/Standards/A36 Acesso 28/04/2016>. Acesso em : 30 de maio de 2018

BAPTISTA, A.L.B.; SOARES, A.R.; NASCIMENTO, I.A.; O Ensaio Metalográfico no Controle da Qualidade. Spectru Ltda - Divisão Instrumental Científico, 2012.

CBCA. A Evolução da Construção em Aço no Brasil. Arquitetura & Aço Available in: < http://www.cbca-acobrasil.org.br/site/noticias-detalhes.php?cod=7074 >. Access at15 jul. 2015.

CULLITY, B. D. Elements of X-ray diffraction. 2.ed. Reading: Addison-Wesley, 1978.

ESTEFEN, S.; GUROVA, T.; CASTELLO, X.; LEONTIEV, A. Conferência de Tecnologia de Soldagem e Inspeção. Análise de Evolução do Estado das Tensões Residuais de Soldagem. Rio de Janeiro, 2008. Available in: <htp://www.gurteq.com/raystress%20download/exposol%202008.pdf>

FERNANDES, PJ. Ensaios Metalográficos. METALOGRAFIA: O que é e para que serve. 2011 Available in < http://profpaulofj.webs.com/oqueeparaqueserve.htm> Access atMaio de 2018

FILHO, H. M. R. L. Análise de Ataques Químicos para Revelação de Microestrutura de Soldas Dissimilares de Aços Inoxidáveis Austeníticos e Ferríticos. FORTALEZA – CE DEZEMBRO, 2013. Available in: <http://www.repositoriobib.ufc.br/000020/0000208e.pdf>

MONINE, V. I., TEODOSIO, J. R., IVANOV. S. A., New Methods of X-Ray Tensiometry. Advances in Experimental Mechanics, v 2, p. 757-761, 1994.

MONINE, V. I., GUROVA, T., ASSIS, J. T., PEREIRA, F. R., SILVA, P. S., "Data processing anda stress measurements by new portable diffractometer", 50th Annual Denver X-Ray Conference, Book of Abstracts, Denver, University, p. 187-197, 2001

PUC-RIO. Tensões Residuais. Available in: <https://www.maxwell.vrac.puc-rio.br/10462/10462_3.PDF> Acesso em 30 de maio de 2018

ROHDE, R A. Metalografia Preparação de Amostras. LEMM Laboratório de Ensaios Mecânicos e Materiais, Outubro 2010 Available in:<http://www.urisan.tche.br/~lemm/metalografia.pdf >. Access at30 de maio de 2018

SÁ, G.M.S.. Estudo da Influência da Composição Química do Metal de Adição na Junta de Aço Inoxidável Super Duplex s32750 (saf2507) Soldada Pelo Processo gtaw (TIG) e Análise de tensões por Soldagem por Difração de Raios X. 2011. Trabalho de Conclusão. Universidade Estadual da Zona Oeste, UEZO, Rio de Janeiro, 2011.